



Comparing fuzzy rule-based and fractional open circuit voltage MPPT techniques in a fuel cell stack

Doudou N. Luta ¹*, Atanda K. Raji ¹

¹ Cape Peninsula University of Technology, Bellville 7535, Western Cape, South Africa

*Corresponding author E-mail: 212123254@mycput.ac.za

Abstract

The concept of power tracking was at first applied to renewable power systems and especially those based on solar and wind to extract as much power as possible from them. Both types of power systems operate on the principle of converting either solar or wind into electricity. Thus, their output power is direct dependent on the solar radiation for solar power systems and on the wind speed for wind generators. To maintain efficient system operations, the output power of these power systems is optimized through maximum power tracking techniques. In the similar vein, fuel cell stacks display nonlinear output powers resulting from internal limitations and operating parameters such as temperature, hydrogen and oxygen partial pressures and humidity levels, etc., leading to a reduced system performance. It is critical to extract as much power as possible from the stack, thus, to prevent also an excessive fuel use. To ensure that, the power converter interfaced to the stack must be able to self-adjust its parameters continuously, hence modifying its voltage and current depending upon the maximum power point position. Diverse techniques are utilized to extract maximum power from the fuel-cell stack. In this paper, a fractional open circuit voltage and fuzzy rule based maximum power tracking techniques are considered and compared. The proposed system consists of a 50 kW Proton Exchange Membrane fuel cell interfaced to a DC-to-DC boost converter. The converter is designed to deliver 1.2 kV from 625 V input voltage. The simulation is carried out under Matlab/Simulink environment.

Keywords: Use about five key words or phrases in alphabetical order, Separated by Semicolon.

1. Introduction

Fuel cells (FCs) are expected to play a key role in the current and future power system model as they are potential candidates to replace fossil fuel-based power generators for clean electricity production. FCs show great capabilities for use in microgrid systems and present advantages such low or nearly zero pollutants gases emission and flexible modular structure [1]. Unlike other green energy technologies such as wind and photovoltaic systems, FCs have the advantage that they can be placed at any site without geographic limitations to provide optimal benefits. [2]. Their operation is such that chemical energy from an electrolytic reaction is continuously converted into electricity in the form of direct current with water and heat as by-products [3]. In this electrolytic reaction, hydrogen serves as the main fuel or reactant while oxygen is the oxidant. However, various other reactants can be used depending upon the FC technology. The most current FC technologies include Proton Exchange or Polymer Electrolytic Membrane Fuel Cell (PEMFC), Phosphoric Acid Fuel Cell (PAFC), Alkaline Fuel Cell (AFC), Molten Carbonate Fuel Cell (MCFC), Solid Oxide Fuel Cell (SOFC) and Direct Methanol Fuel Cell (DMFC) [3–5]. A common FC stack displays a nonlinear power output as a result of internal limitations and operating parameters including the temperature, hydrogen and oxygen partial pressures, hydrogen and oxygen humidity levels, hydrogen and oxygen gases speed and stoichiometry, and membranes water content [1,6,7], leading to a reduced system performance. It is critical to extract as much power as possible from the stack as at all the operating conditions, there is only one maximum power point in the power versus current (P-I) FC curve. This allows preventing an excessive fuel use and avoiding low system efficiency. To ensure that, a switch mode power converter known as maximum power point tracker (MPPT) is interfaced between the FC and the load and operates such that the converter's duty cycle is adjusted continuously, hence modifying the voltage and current depending upon the maximum power point position. If a proper algorithm is used, the MPPT will be able to locate and track the FC MPP.

As of now, diverse techniques are utilised to extract maximum power [8-11]. Most of these techniques are used for photovoltaic and wind generators [12, 8] and vary from each other in several respects such as efficiency, convergence speed, complexity, sensors needed, cost, hardware implementation and many other aspects. [9] classified these methods in five categories listed in Table 1.

Table 1: Maximum Power Point Methods

MPPT techniques and methods	MPPT methods
MPPT techniques	Constant voltage method
1 Methods using predefined values characterising the Maximum Power Point	Open-circuit voltage method
	Short-circuit current method



		Open-circuit voltage pilot PV cell method Temperature Gradient algorithm Temperature parametric method Feedback voltage or current method P-N junction drop voltage tracking technique
2	Method sensing the external parameters such as voltage, current etc., and comparing them with the pre-known values characterising the Maximum Power Point	Look-up table method Load current or load voltage maximisation Linear current control method
3	Method based on attempting to calculate and observe the result to determine the direction criteria for the next attempt to get to the Maximum Power Point	Only-current photovoltaic method PV Output Senseless control method Perturb and Observe method Three-point weight comparison method On-Line Maximum Power Point search method DC-Link capacitor droop control Array Reconfiguration method Maximum Power Point Tracking with variable inductorlevel-2 heading, left-justified
4	Method defining the Maximum Power Point based on mathematical calculation using available data	State-based Maximum Power Point Tracking method Linear reoriented coordinates method Curve-fitting method Differentiation method Slide control method Current sweep method dP/dV or dP/dI feedback control Incremental Conductance method Parasitic capacitance method Maximum Power Point Current and voltage computation method β method Methods by modulation Ripple correlation control
5	Method using intelligent learning process	Fuzzy logic method Neural network method Biological swarm chasing algorithm

This paper investigates two MPPT controllers; one based on Fuzzy inference system using Sugeno method and another one is adapted from Fractional Open Circuit Voltage technique, the objective is to compare both controllers' performances in terms of their response characteristics. The investigation is conducted on a 50 kW Proton Exchange Membrane Fuel Cell stack coupled to a power electronics converter and a DC load. The simulation is carried out under Matlab/Simulink environment. The remaining of the paper is organised as follows, the next section is dedicated to the system description, modelling, section 3 gives the simulation results, and the last section deals with the conclusion.

2. System modelling

The proposed system (Fig. 1) consists of a 50 kW Proton Exchange Membrane Fuel cell (PEMFC) stack, a DC-to-DC boost converter and a MPPT controller. The voltage and current of the fuel cell stack are sensed and used as inputs to the MPPT controller, which in turn delivers a signal for the PWM generator to drive the boost converter switch. The converter is designed to deliver 1.2 kV from a 625 V input voltage.

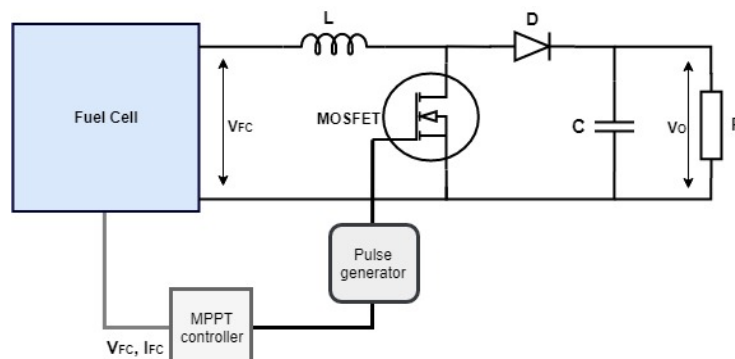
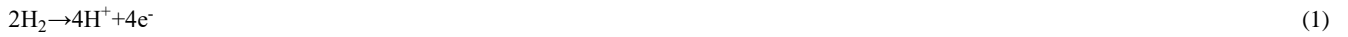


Fig. 1: System Modelling.

2.1. Characteristics of PEMFC

In a PEMFC, hydrogen and oxygen are combined in cells to generate electricity with water and heat as by-products. A simple analogy to be made with FCs as opposed to batteries is that the reactants are continuously supplied in FCs while batteries reactants are finite. At the anode of a PEMFC, hydrogen gas ionises freeing electrons and creating H⁺ as shown in (1), in the meantime, at the cathode, oxygen reacts with electrons extracted from the electrode, and H⁺ from the electrolyte to form water as expressed in (2) [3].



The general reaction happening in a FC follows (3) given as [13]:



The FC model adopted in this investigation is a modified version of the approach proposed by [14], whereby the dynamics of the reactant flow are ignored.

The voltage generated from the electro-chemical reactions is expressed by the Nernst equation as:

$$E_n = 1.229 + (T - 298) \cdot \frac{-44.43}{2F} + \frac{RT}{2F} \ln \left(P_{\text{H}_2} P_{\text{O}_2}^{\frac{1}{2}} \right) \quad (4)$$

Where P_{H_2} and P_{O_2} are the hydrogen and oxygen partial pressures respectively, T is the temperature, F is the Faraday constant and R the ideal gas constant.

The partial pressures are defined as function of reactant utilisation in (5) and (6) as follows:

$$P_{\text{H}_2} = (1 - U_{f_{\text{H}_2}}) x \% P_{\text{fuel}} \quad (5)$$

$$P_{\text{O}_2} = (1 - U_{f_{\text{O}_2}}) y \% P_{\text{air}} \quad (6)$$

Where $U_{f_{\text{H}_2}}$ and $U_{f_{\text{O}_2}}$ are the hydrogen and oxygen utilisation respectively, P_{fuel} and P_{air} are the supply pressures of the hydrogen and oxygen respectively, x and y are the percentages of hydrogen and oxygen compositions.

The rates of reactant utilisation are given as follows:

$$U_{f_{\text{H}_2}} = \frac{60000RT_{f_c}}{2FP_{\text{hydr}}V_{\text{hydr}}x\%} \quad (7)$$

$$U_{f_{\text{O}_2}} = \frac{60000RT_{f_c}}{4FP_{\text{oxyg}}V_{\text{oxyg}}y\%} \quad (8)$$

Where V_{fuel} and V_{air} are the hydrogen and oxygen flow rates, i_{f_c} is the cell current

The absence of oxygen in the cell leads to the increase of its utilisation over the nominal value; hence (4) is adjusted as:

$$E_n = 1.229 + (T - 298) \cdot \frac{-44.43}{2F} + \frac{RT}{2F} \ln \left(P_{\text{H}_2} P_{\text{O}_2}^{\frac{1}{2}} \right) - K_u \left(U_{f_{\text{O}_2}} - U_{f_{\text{O}_2\text{nom}}} \right) \quad (9)$$

Where K_u is the voltage undershoot constant and $U_{f_{\text{O}_2\text{nom}}}$ is the nomination oxygen utilisation

The open circuit voltage of a single cell is given in (10) as follows:

$$E_o = K_C E_n \quad (10)$$

Where K_C is the voltage constant

Taking into consideration losses including the activation losses, and resistive and diffusion losses, the open circuit voltage of a single cell is expressed as:

$$V = E_o - V_{\text{act}} - V_r \quad (11)$$

$$\text{Whereby: } V_{\text{act}} = A \ln \left(\frac{i_{f_c}}{i_o} \right) \cdot \frac{1}{S \frac{T_d}{3} + 1} \quad (12)$$

$$V_r = r_{\text{ohm}} \cdot i_{f_c} \quad (13)$$

Where T_d is the cell settling time to a current step and r_{ohm} is the cell resistance,

$$A = \frac{RT}{2\alpha F} \quad (14)$$

$$\text{and } i_o = \frac{2Fk(P_{\text{H}_2} + P_{\text{O}_2})}{R_h} \cdot \exp \left(\frac{\Delta G}{RT} \right) \quad (15)$$

Where α is the charge transfer coefficient, ΔG is the activation energy barrier, k is the Boltzmann constant and h is the Plank constant.

The complete FC stack voltage is given as follows:

$$V_{f_c} = N \cdot V \quad (16)$$

Where N is the number of cells in the stack

The polarisation curve of the FC considered in this study is displayed in Fig.2, it is based on equations (4) to (16) using parameters in Table 2.

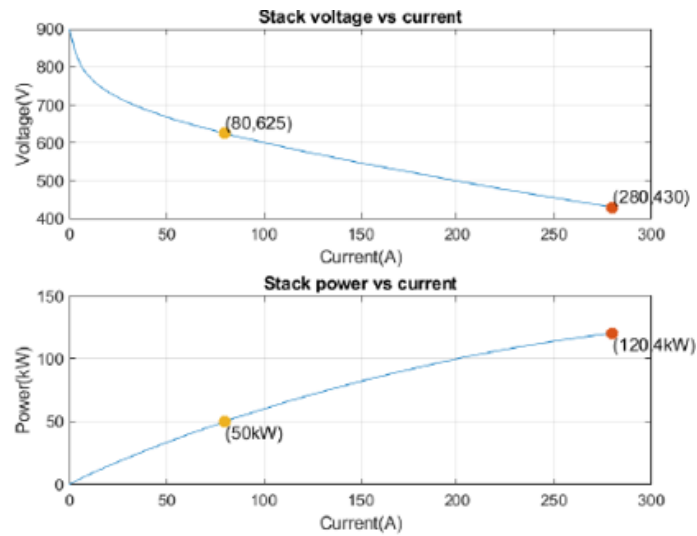


Fig. 2: 50 kW FC Stack Polarisation Curves.

Table 2: FC Model Parameters

Model input parameters for 50 kW FC stack	
Voltage at 0 A and 1A	900 V and 895 V
Nominal operating point	80 A and 625 V
Maximum operating point	280 A and 430 V
Number of cells	900
Nominal stack efficiency	55 %
Operating temperature	338 °K
Nominal air flow rate	2100 litre per minute
Nominal supply pressure	1.5 bar for the hydrogen and 1 bar for the oxygen
Nominal composition	99.95% for the hydrogen, 21% for the oxygen and 1% for water
Voltage response time	1 second

2.2. DC-to-DC booster converter

In a boost converter (Fig. 1), an unregulated voltage is converted into desired regulated voltage by readjusting the duty cycle at high switching frequency. The choice of components such as the inductor and capacitor is crucial to decrease the ripple generation for a given switching frequency. In a continuous conduction mode, a boost converter operates for L greater than L_C defined as:

$$L_C = \frac{(1-D)^2 \cdot D \cdot R}{2 \cdot f} \tag{17}$$

Whereby $D = \frac{V_O - V_{FC}}{V_O}$ (18)

Where f is the switching frequency and R is the load

To hinder high ripple voltage, a boost converter requires a filter capacitor as the current supplied to the RC circuit is discontinuous. Whenever the diode is turned off, the capacitor supplies the output current. Thus, the capacitor must be higher than a certain value. The minimum value of the capacitor C_{Min} is expressed as:

$$C_{Min} = \frac{V_O \cdot D}{\Delta V_O \cdot f \cdot R} \tag{19}$$

Where ΔV_O is the ripple voltage

In this study, a boost converter operating at a switching frequency of 30 kHz is designed to step-up a 625 V dc voltage of the fuel cell to 1.2 kV. Table 3 gives the design parameters of the converter.

Table 3: Converter Parameters

Boost converter parameters	
Inductance	2.9x10 ⁻³ H
Capacitor	70x10 ⁻⁶ F
Switching frequency	30 kHz
Input voltage	625 V
Output voltage	1.2 kV
Efficiency	90 %
Load	28.8 Ω

3. Maximum power point controller simulation and results

3.1. Fractional open circuit voltage method

The fractional open circuit voltage MPPT method is one of the simplest, easy to implement and has low complexity as compared to others. It derives from the fact that the MPP voltage is continuously a proportion of the open circuit voltage as expressed in (20):

$$V_{MPP} = K_v V_{op} \quad (20)$$

Where V_{MPP} is the maximum power point voltage, K_v is the voltage factor and V_{op} is the open circuit voltage

The voltage factor (K_v) is inconstant and always dependent on the temperature variation. V_{MPP} is often estimated through the measurement of the open circuit voltage of the FC stack, the measured value is then multiplied by the voltage factor. The measurement can be carried out on a regular basis after a certain interval of time and necessitates that the load must be disconnected from the stack, thus causing the loss of power supply for the load. The precision of measured V_{op} often depends on the duration and the frequency of measurement as high frequency and longer measurement can provide an accurate V_{MPP} estimation. For PV panels, typical values for K_v depend on the type of the panel and its characteristics, however, regardless of the type, these values range from 0.73 to 0.8 [15], [16].

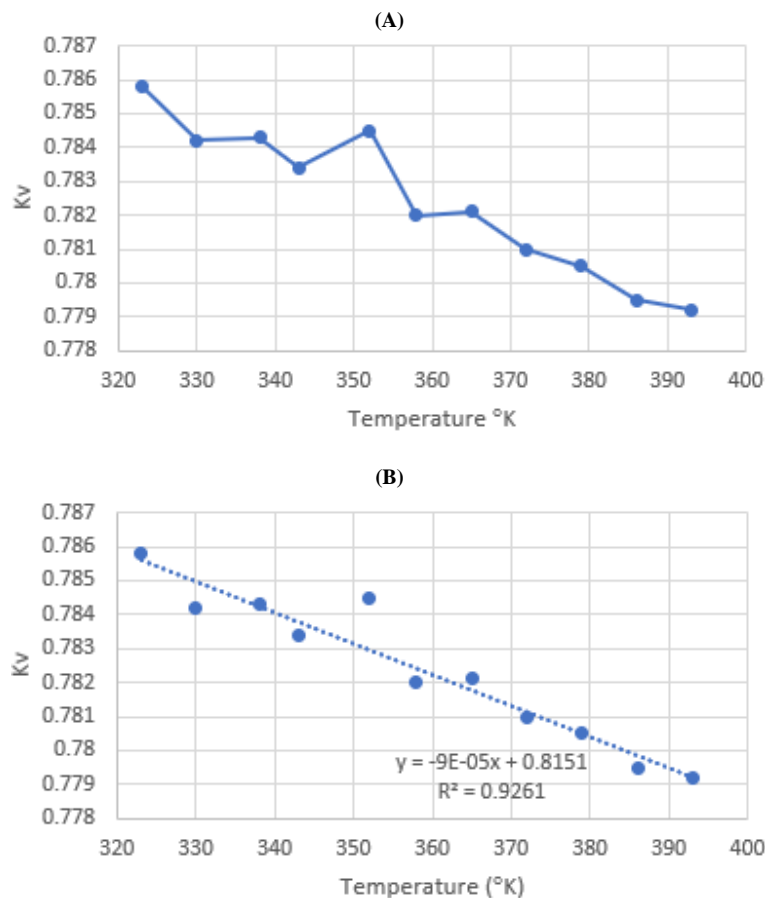


Fig. 3: (A) And (B) Fitting Line K_v As Function of Temperature.

[17] proposed the values of K_v for PEMFC as function of the temperature variation (see Figure 3(a)). The operating temperature of the PEMFC considered is 338° K (Table 1), thus, the corresponding value K_v is between 0.783 and 0.785 (Fig. 3). The estimated value of K_v is obtained using the curve fitting process as shown in Fig. 3. The fitting line to determine the value of K_v corresponding to the considered fuel cell is given in (21) as:

$$y = -9.10^{-5} \cdot x + 0.8151 \quad (21)$$

Where y represents K_v and x is the temperature.

Therefore, using (21) and the operating temperature of the PEMFC used which is 338° K, K_v is determined as 0.78468.

Based on the model in Fig. 4, a simulation was carried out to obtain the output curves of the voltage, current and power. The model includes a fuel cell stack, a fractional open-circuit voltage MPPT controller, a boost converter with a pulse width modulation that receive its duty cycle from the MPPT controller. The converter components sizes are determined based on the values in Table 3. The fuel cell voltage operating voltage and open circuit voltage, which is 900 V (Table 2) are used as inputs to the MPPT controller. At the same time, the fuel cell is connected to the load through the converter. The hydrogen and oxygen consumptions in the fuel cell are assumed to be unchanged throughout the simulation and the results are shown in Fig. 5.

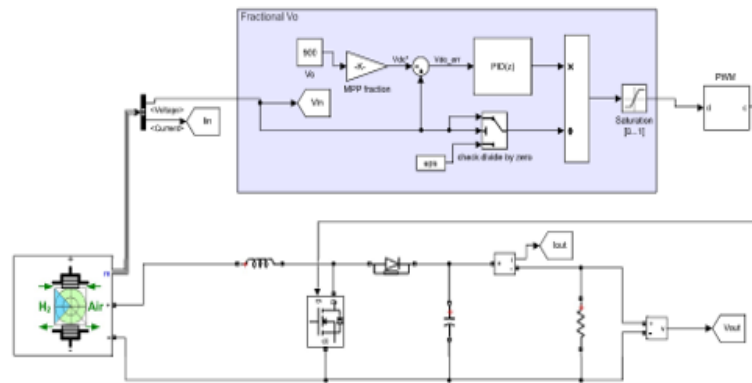
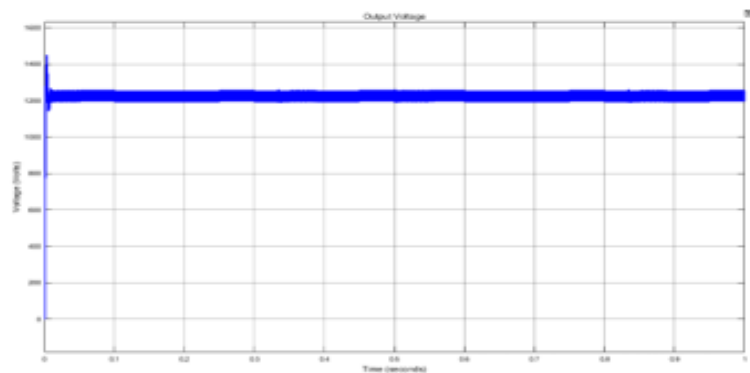


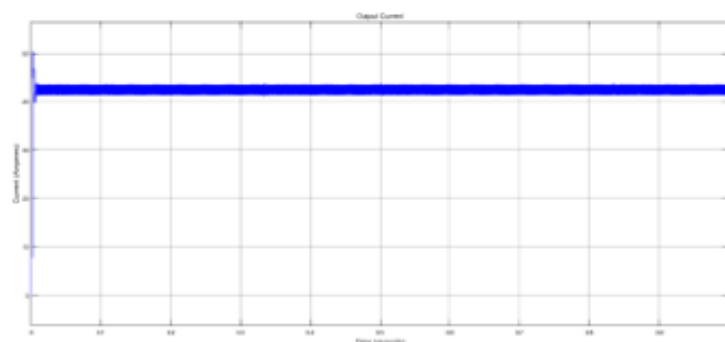
Fig. 4: System Model with Fractional Open Circuit Voltage Controller.

The output voltage of the system at the load side is about 1.232 kV as shown in Figure 5a, the fuel cell hydrogen flow rate, hydrogen pressure and temperature being unchanged, the operating voltage is as well at a constant value. It has a rising time of about 1.306 ms, which corresponds to the time required for the voltage to rise from 0 to 100% of its final value. In addition, the overshoot and undershoot are 17.059% and 7.578% respectively. These percentages of undershoot and overshoot show the appearance of the signal exceeding 1.232 kV and the occurrence of the signal below 1.232 kV respectively.

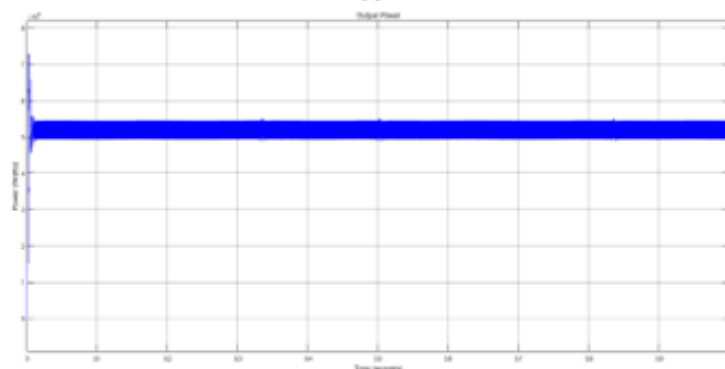
The output current at the terminals of the converter is shown in Figure 5b and has a value of about 42.79 A, it has a rising time of about 1.306 ms, and an overshoot and undershoot of 17.059% and 7.578% respectively. In the same vein, the power at the terminals of the converter is displayed in Figure 5c, and corresponds to 53.28 kW, its rising time is 1.236 ms, with an overshoot and undershoot of 36.301 % and 14.355% respectively. Its settling time which refers to time required for the power curve to reach and stay within a range about its final value by absolute percentage of its final value (usually 2% or 5%) is 19.983 ms.



(a)



(b)



(c)

Fig. 5: (A) Output Voltage, (B) Output Current and (C) Output Power Using Fractional Open Circuit Voltage MPPT Controller.

3.2. Fuzzy rule-based method

Fuzzy logic is used in a wide range of applications; controllers based on fuzzy logic are recognised for being robust and simple to design as they do not necessitate precise knowledge of the model of the system to be controlled. They consist of an input, a processing phase and an output.

For MPPT controller design, two inputs are required namely the error e and the change in error Δe . The error is expressed as:

$$e(k) = \frac{p(k) - p(k-1)}{v(k) - v(k-1)} \quad (22)$$

Where $p(k)$, $p(k-1)$, $v(k)$ and $v(k-1)$ are the powers and voltages at instant k and $k-1$ respectively

The change in error Δe_k is given as follows:

$$\Delta e_k = e_k - e_{k-1} \quad (23)$$

Where e_k and e_{k-1} are the error at instant k and $k-1$ respectively.

The processing phase also known as inference engine is based on logical rules containing IF-THEN statements. Common fuzzy inference systems include dozens of rules [18]. The inference engine processes the given input values to generate the outputs based on the defined rules. Five different steps are involved namely fuzzification, application of fuzzy operator, application of implication method, aggregation of outputs and defuzzification [18].

Fuzzy inference systems are based on two methods: Mamdani fuzzy inference method [19] and Takagi-Sugeno-Kang inference method [20]. The major different between them lies in the consequent fuzzy rules and defuzzification procedures; Mamdani inference method uses fuzzy sets as rule consequent, while Sugeno inference method considers linear functions of input variables. In Mamdani approach, the crisp output of the fuzzy system y^{crisp} is determined using the "Centre of Gravity" defuzzification by supposing that the consequent fuzzy set of Rule i is Q^i , characterised by membership u^{Q^i} and by defining the centre of areas of u^{Q^i} to be the point q_i in the universe. Equation (24) gives the crisp output of Mamdani method [21]:

$$y^{crisp} = \frac{\sum_{i=1}^R q_i \int u^{Q^i}}{\sum_{i=1}^R \int u^{Q^i}} \quad (24)$$

In the same vein, the crisp output of Sugeno fuzzy systems is given as [21]:

$$y^{crisp} = \frac{\sum_{i=1}^R q_i u_i(\underline{x})}{\sum_{i=1}^R u_i(\underline{x})} \quad (25)$$

Where $u_i(\underline{x})$ is the premise membership value of Rule i

Between the two methods, Mamdani inference system is the most widely used as it presents some benefits such as (Hamam and Georganas, 2008): intuitive and interpretable nature of the rule base, easy formalisation and interpretability, expressive power and able to be employed in both MISO and MIMO systems. The advantage of Sugeno inference method is as follows (Subhedar and Birajdar, 2013): computational accuracy and efficiency, better processing time and adequate for functional analysis. In this study, a Sugeno type fuzzy inference engine is proffered over the Mamdani type.

The proposed Sugeno fuzzy logic controller uses two inputs shown in Figure 6a, each input consists of five triangular membership functions with a normalised universe of discourse ranging from -2 to 2. These inputs are the error and the change in error as expressed in (21) and (22). They include five variables namely negative big (NB), negative small (NS), zero (Z), positive small (PS) and positive big (PB). The rules are designed based on the provided inputs and the surface viewer in Figure 6b shows the relationship between the inputs and output. It is considered that both fuzzy inference engines use the same rules.

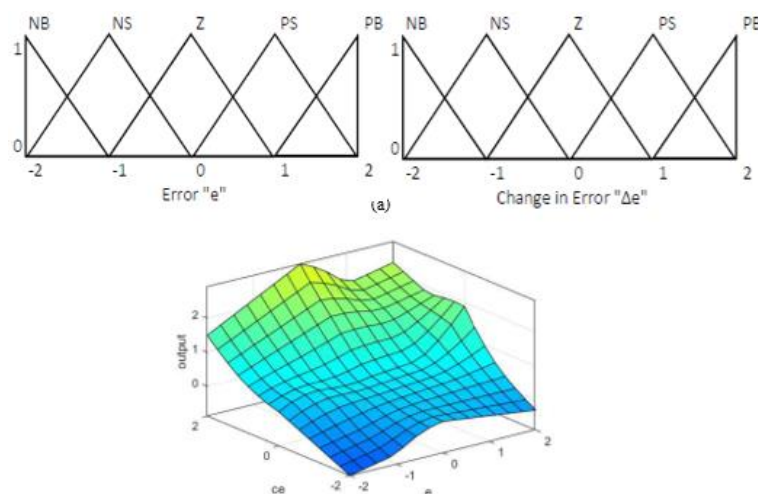


Fig. 6: A) Input Membership Functions, B) Rule Surface Viewer.

The output of Sugeno inference engine consists of five linear membership functions which are negative big (NB) located at [-0.1667 0.125 0.2917], negative small (NS) at [0.125 0.2917 0.5], zero (Z) at [0.2917 0.5 0.7083], positive small (PS) at [0.5 0.7083 0.875] and positive big (PB) at [0.7083 0.875 1.167].

The system depicted in Fig. 7 was simulated under Matlab/Simulink environment. Sugeno fuzzy logic controller based on characteristics shown in Fig. 6 replaced the fractional; open-circuit voltage MPPT controller. The hydrogen and oxygen consumptions in the fuel cell are assumed unchanged throughout the simulation and the results are shown in Fig. 8.

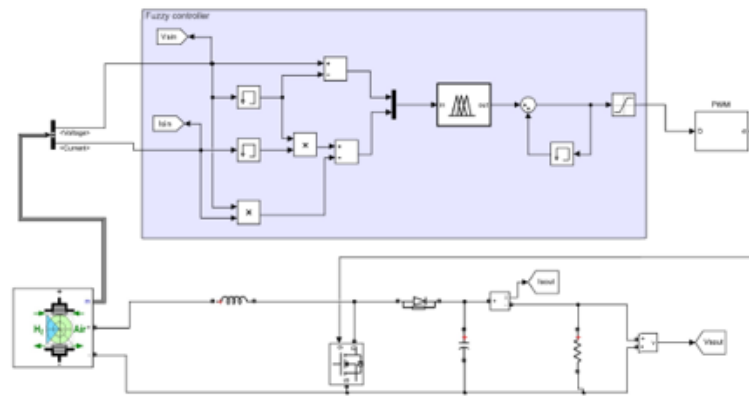


Fig. 7: System Model with Sugeno Fuzzy Controller.

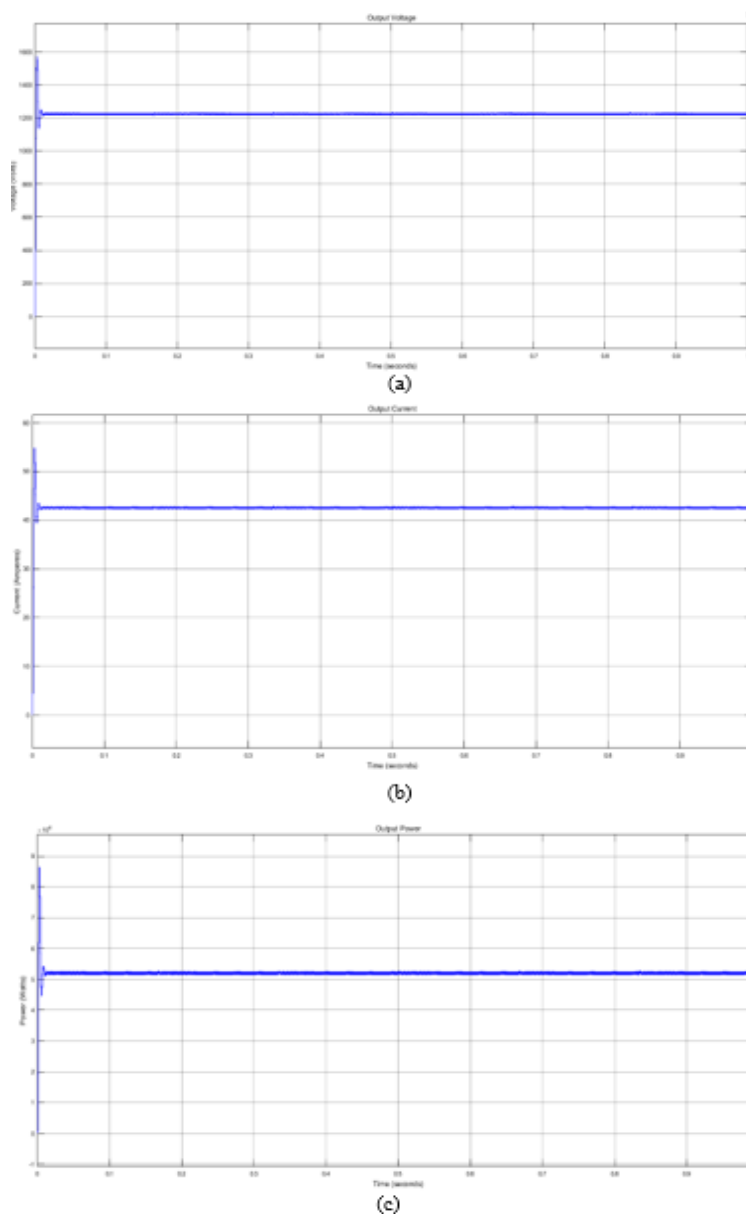


Fig. 8: (A) Output Voltage, (B) Output Current and (C) Output Power Using Sugeno Fuzzy Logic MPPT Controller.

The output voltage at the terminals of the converter is about 1.214 kV (see Figure 8a), the fuel cell hydrogen flow rate, hydrogen pressure and temperature being unchanged, this voltage is constant throughout the simulation. The voltage has a rising time of about 1.172 ms. In addition, the overshoot and undershoot are 29.221% and 5.816% respectively. The time that this voltage requires to reach and stay within a range of its final value is about 8.072 ms.

Similarly, the output current of this system is shown in Figure 8b and has a value of about 42.17 A, it has a rising time of about 1.172 ms, and an overshoot and undershoot of 29.221% and 5.816% respectively. The rising time corresponding to the output current is 8.072 ms. In the same vein, the power at the terminals of the converter is displayed in Figure 5c, and is around 51.83 kW, its rising time is 892.288 μ s, with an overshoot and undershoot of 65.833% and 1.121% respectively, while the settling time is 10.53 ms.

3.3. Comparison between open circuit voltage MPPT and sugeno fuzzy logic MPPT methods

The overall results illustrated in Table 4 show better performance of the Sugeno-type controller over Fractional Open Circuit Voltage controller; concerning the voltage, Sugeno-type controller presents an average voltage of 1214 V which 1.01% higher than the converter calculated voltage of 1200 V, whereas the Fractional Open Circuit Voltage controller voltage is 1.0268% slightly higher. The rising time of Sugeno controller is faster than the Fractional controller as it is about 1.172 ms, while that of the Fractional controller is 1.306 ms. However, Sugeno controller shows an overshoot of 29.221% compared to the Fractional Open Circuit Voltage controller which is lower and equal to 17.059%. The corresponding values of undershoots are such that the Sugeno controller has a lower undershoot of 5.816% and Fractional Open Circuit Voltage is 7.578%. The output voltage of Sugeno controller settles at time $t=8.072$ ms whereas that of the Fractional Open Circuit Voltage does not settle during the simulation.

Similarly, Sugeno-type controller presents an average current of 41.17 A which 1.029% higher than the converter calculated current of 40 A, whereas the Fractional Open Circuit Voltage controller current is 1.068%. The rising time of Fractional Open Circuit Voltage controller is faster than the Sugeno controller as it is about 398.196 μ s, while that of Sugeno controller is 1.172 ms. However, Sugeno controller shows an overshoot of 29.221% compared to the Fractional Open Circuit Voltage controller which is lower and equal to 17.059%. The corresponding values of undershoots are such that the Sugeno controller has a lower undershoot of 5.816% and Fractional Open Circuit Voltage is 7.578%. the output current proposed by Sugeno controller settles at time $t=8.072$ ms whereas that of the Fractional Open Circuit Voltage does not settle during the simulation.

In the same vein, Sugeno-type controller presents an average power of 51.83 kW which 1.0366% higher than the calculated power, whereas the Fractional Open Circuit Voltage controller power is 1.0656%. The rising time of Fractional Open Circuit Voltage controller is lower than Sugeno controller as it is about 1.236 ms, while that of Sugeno controller is 896.288 μ s. Sugeno controller shows an overshoot of 65.833% and the Fractional Open Circuit Voltage controller overshoot is 36.301%. The corresponding values of undershoots are such that the Sugeno controller has a lower undershoot of 1.121% and Fractional Open Circuit Voltage is 14.355%. The output power proposed by Sugeno controller settles at time $t=10.53$ ms whereas that of the Fractional Open Circuit Voltage settling time is 19.983 ms.

Table 4: Comparison between Open Circuit Voltage and Sugeno Fuzzy controllers

Comparison	Fractional Open Circuit Voltage controller	Fuzzy logic based Sugeno controller
Voltage		
Average	1232 V	1214 V
Rise Time	1.306 ms	1.172 ms
Overshoot	17.059%	29.221%
Undershoot	7.578%	5.816%
Settling time	-	8.072 ms
Current		
Average	42.71 A	42.17 A
Rise Time	398.196 μ s	1.172 ms
Overshoot	17.059%	29.221%
Undershoot	7.578%	5.816%
Settling time	-	8.072 ms
Power		
Average	53.28 kW	51.83 kW
Rise Time	1.236 ms	896.288 μ s
Overshoot	36.301%	65.833%
Undershoot	14.355%	1.121%
Settling time	19.983 ms	10.53 ms

4. Conclusion

Maximum power extraction concept was first applied to photovoltaic panels to optimize their output power, as there are weather dependent. It is achieved by displacing the photovoltaic voltage or current through a switching converter to obtain the maximum power. Fuel cells are also candidate for maximum power extraction as their operation is influenced by some internal limitation such as temperature, hydrogen and oxygen partial pressures, hydrogen and oxygen humidity levels, hydrogen and oxygen gases speed and stoichiometry, and membranes water content. At every instant, the system needs to be constrained to deliver as maximum power as possible thus avoiding low efficiency. Various methods can be employed for MPPT controllers design and each has its benefits, specifications and drawbacks. This paper investigated MPPT controllers based on fuzzy inference engine using Sugeno method and Fractional Open Circuit Voltage, the objective was to compare both controllers in terms of response characteristics. The investigation was conducted on a 50 kW PEMFC stack coupled to a power electronics converter and a DC load. The converter was designed to boost 625 V input of the fuel cell to 1.2 kV. The modelling And simulation was carried out using Matlab/Simulink. The overall results show better performance of the Sugeno-type controller over the Fractional Open Circuit Voltage controller.

References

- [1] Caisheng W, Nehrir MH, Shaw SR. Dynamic models and model validation for PEM fuel cells using electrical circuits. *IEEE Trans Energy Convers* 2005;20:442–51. <https://doi.org/10.1109/TEC.2004.842357>.
- [2] Nehrir MH, Caisheng W, Shaw SR. Fuel cells: promising devices for distributed generation. *Power Energy Mag IEEE* 2006;4:47–53. <https://doi.org/10.1109/MPAE.2006.1578531>.
- [3] Larminie J, Dicks A. *Fuel cell systems explained*. 2nd ed. John Wiley & Sons Ltd; 2003. <https://doi.org/10.1002/9781118878330>.
- [4] Revankar S, Majumdar P. *Fuel Cells: Principles, Design and Analysis*. CRC Press; 2014.

- [5] Luta DN, Raji AK. Decision-making between a grid extension and a rural renewable off-grid system with hydrogen generation. *Int J Hydrogen Energy* 2018;43:1–14. <https://doi.org/10.1016/j.ijhydene.2018.04.032>.
- [6] Harrag A, Messalti S. How fuzzy logic can improve PEM fuel cell MPPT performances? *Int J Hydrogen Energy* 2018;43:537–50. <https://doi.org/10.1016/j.ijhydene.2017.04.093>.
- [7] Mann RF, Amphlett JC, Hooper M a. I, Jensen HM, Peppley B a., Roberge PR. Development and application of a generalised steady-state electrochemical model for a PEM fuel cell. *J Power Sources* 2000;86:173–80. [https://doi.org/10.1016/S0378-7753\(99\)00484-X](https://doi.org/10.1016/S0378-7753(99)00484-X).
- [8] Esram T, Chapman PL. Comparison of Photovoltaic Array Maximum Power Point Tracking Techniques. *IEEE Trans Energy Convers* 2007;22:439–49. <https://doi.org/10.1109/TEC.2006.874230>.
- [9] Karami N, Moubayed N, Outbib R. General review and classification of different MPPT Techniques. *Renew Sustain Energy Rev* 2017;68:1–18. <https://doi.org/10.1016/j.rser.2016.09.132>.
- [10] Eltawil MA, Zhao Z. MPPT techniques for photovoltaic applications. *Renew Sustain Energy Rev* 2013;25:793–813. <https://doi.org/10.1016/j.rser.2013.05.022>.
- [11] Ram JP, Babu TS, Rajasekar N. A comprehensive review on solar PV maximum power point tracking techniques. *Renew Sustain Energy Rev* 2017;67:826–47. <https://doi.org/10.1016/j.rser.2016.09.076>.
- [12] Kumar D, Chatterjee K. A review of conventional and advanced MPPT algorithms for wind energy systems. *Renew Sustain Energy Rev* 2016;55:957–70. <https://doi.org/10.1016/j.rser.2015.11.013>.
- [13] Barbir F. PEM fuel cells : theory and practice. 2013. <https://doi.org/10.1016/B978-0-12-387710-9.01001-8>.
- [14] Pukrushpan JT, Stefanopoulou AG, Peng H. *Control of Fuel Cell Power Systems": Principles, Modeling, Analysis and Feedback Design*. Springer Verlag London; 2006. <https://doi.org/10.1007/978-3-319-08413-8>.
- [15] Hohm DP, Ropp ME. Comparative study of maximum power point tracking algorithms using an experimental, programmable, maximum power point tracking test bed. *Photovolt. Spec. Conf. 2000. Conf. Rec. Twenty-Eighth IEEE, Anchorage, Alaska, USA: IEEE; 2000, p. 1699–702*. <https://doi.org/10.1109/PVSC.2000.916230>.
- [16] Onat N. Recent developments in maximum power point tracking technologies for photovoltaic systems. *Int J Photoenergy* 2010;2010. <https://doi.org/10.1155/2010/245316>.
- [17] Sarvi M, Barati M. Voltage and current based MPPT of fuel cells under variable temperature conditions. *Univ. Power Eng. Conf.*, vol. 2, 2010, p. 2–5.
- [18] Blej M, Azizi M. Comparison of Mamdani-Type and Sugeno-Type Fuzzy Inference Systems for Fuzzy Real Time Scheduling 2016;11:11071–5.
- [19] Mamdani E., Assilian S. An Experiment in Linguistic Synthesis with a Fuzzy Logic Controller. *Int J Hum Comput Stud* 1999;51:135–47. <https://doi.org/10.1006/ijhc.1973.0303>.
- [20] Takagi T, Sugeno M. Fuzzy identification of systems and its applications to modeling and control. *Syst Man Cybern IEEE Trans* 1985;SMC-15:116–32. <https://doi.org/10.1109/TSMC.1985.6313399>.
- [21] Lilly JH. *Fuzzy Control and Identification*. Wiley & Sons Ltd; 2010. <https://doi.org/10.1002/9780470874240>.